Effect of Modified Layered Silicates on the Confined Crystalline Morphology and Thermomechanical Properties of Poly(ethylene oxide) Nanocomposites

T. N. Abraham,[1] S. Siengchin,[2] Debdatta Ratna,[3] J. Karger-Kocsis[4]

[1]*Defence Laboratory, Ratanada Palace, Jodhpur 342011, India*
[2]*The Sirindhorn International Thai-German Graduate School of Engineering, King Mongkut's University of Technology North Bangkok, Bangsue, Bangkok 10800, Thailand*
[3]*Naval Materials Research Laboratory, Additional Ambernath, Thane 421506, India*
[4]*Polymer Technology, Faculty of Mechanical Engineering and Built Environment, Tshwane University of Technology, Pretoria, South Africa*

Received 19 December 2009; accepted 19 February 2010
DOI 10.1002/app.32307
Published online 3 June 2010 in Wiley InterScience (www.interscience.wiley.com).

ABSTRACT: In this work, poly(ethylene oxide) (PEO)/organoclay nanocomposites with three different types of nanoclays (Cloisite 30B, Somasif JAD400, and Somasif JAD230) were prepared by melt mixing with a laboratory kneader followed by compression molding. The nanocomposites were characterized by atomic force microscopy and scanning electron microscopy. Their crystallization behavior on a hot stage was investigated with polarized optical microscopy. The size and regularity of the spherulites of the PEO matrix were altered significantly by the incorporation of Cloisite 30B, but there was not as much variation with the other two clays. The dynamic viscoelastic behavior of the PEO/organoclay nanocomposites was assessed with a strain-controlled parallel-plate rheometer. The effects of clay modification on the thermomechanical and rheological properties were addressed. The reinforcing effect of the organoclay was determined with dynamic mechanical analysis and tensile testing. © 2010 Wiley Periodicals, Inc. J Appl Polym Sci 118: 1297–1305, 2010

Key words: nanocomposites; organoclay; poly(ethylene oxide); viscoelastic

INTRODUCTION

Nanocomposites, a new class of composites, are particle-filled polymers for which at least one dimension of the dispersed particles is nanoscale (1–100 nm). For a nanocomposite system, fundamentally new properties typically originate from changes in the nature of the polymer in the vicinity of the filler, such as polymer adsorption on the filler surfaces or confinement between fillers; as such, they depend strongly on the effective surface area of the filler. The basic principle behind the formation of polymer nanocomposites (PCNs) is that the polymer should intercalate into the galleries of the clay. When the polymer molecules intercalate into the silicate gallery, there is a decrease in entropy that is compensated by either an increase in entropy in the organic modifiers used to widen the gallery spacing or an enthalpic term arising from the intercalation of the polymer and organically modified clay layers.[1–3] The nanocomposite structure depends on the nature of the polymer,[4,5] the organic modifier,[1,5,6] and the processing conditions.[7,8] Effective exploitation of PCNs requires an understanding of the nanoscale structure–property–processing relationships.

Poly(ethylene oxide) (PEO) is a semicrystalline polymer that has been considered in recent years for important applications, such as biomedical[9] and electrochemical applications[10–12] and crystallizable switching segments for shape-memory polymer systems.[13–15] The common problem for all these applications is the poor mechanical properties of PEO. In addition, conventional PEO-based solid polymer electrolytes exhibit low ionic conductivity that is insufficient for many applications. The incorporation of layered silicates is known to improve the mechanical properties and increase the conductivity of PEO-based electrolytes as the silicate layers act as anions and hence the cations can preferentially move.[15,16]

Since Aranda and Ruiz-Hitzky[17] reported the preparation of PEO/clay nanocomposites (PEOCNs) by solution intercalation, much work has been done in this area.[18–23] The preparation of nanocomposites has been demonstrated with pristine clay (in an aqueous intercalant solution) and organophilic clay with polar intercalents[18,19] (Cloisite 30B) and apolar

Correspondence to: T. N. Abraham (thomasnabraham@gmail.com).

intercalents[20,21] (Nanochore I-30). Because PEO is a hydrophilic polymer and is soluble in water, nanocomposites can be made with pristine clays.[22,23] Choi and coworkers[24] correlated the rheological properties to the mesoscopic structure, and it was postulated that the molecular weight and interaction strength would affect the mesoscopic structure and rheological properties of these nanocomposites. The relative mobility of bulk and interphase polymers in intercalated PEOCNs was determined with rheological experiments,[24,25] nuclear magnetic resonance,[26] and neutron scattering.[27] Chen and Evans[28] reported comparative sorption experiments for the molar mass in PCNs, and the results showed that high-molar-mass fractions of the polymer intercalated preferentially into smectite clay with a solution-intercalation method. Bonderer et al.[29] compared the mechanical properties of artificial composites reinforced with submicrometer-thick alumina platelets with clay-based nanocomposites. Loizou et al.[30] studied the dynamic responses of PEO nanocomposite hydrogels. Recently, we reported the optimization of processing parameters based on the rheological properties of PEOCNs made via melt mixing.[31]

PEOCNs can be successfully made with pristine clay by a solution-intercalation method with a polar solvent such as water. However, the melt mixing of PEO and pristine clay leads to the formation of a microcomposite. Nanocomposite can be made only with an organically modified clay. The organic modification of clay serves two purposes: it introduces hydrophobic character into the gallery and enhances the *d*-spacing. Both features encourage the polymer interaction leading to the formation of a nanocomposite.

Studies of PEOCNs (made by melt mixing) have mostly used Cloisite 30B. There is no report on a detailed study of the effect of the nature of the clay modifier on the properties of nanocomposites. The aim of this work was to study the role of an onium salt, which is structurally similar to PEO. In this work, we propose the melt mixing of PEOCNs with three different types of clays: Cloisite 30B, Somasif JAD400, and Somasif JAD230. Somasif JAD has a poly(ether amine)-bound anion that is structurally similar to PEO. Hence, we expected a Somasif-based nanocomposite to behave differently than Cloisite 30B-based nanocomposite. The rheological and dynamic properties and morphology of PEOCNs made with the different clays are discussed.

EXPERIMENTAL

Materials

A PEO matrix with a weight-average molecular weight of 100,000 g/mol was purchased from Acros Organics (Geel, Belgium). An organophilic clay (Cloisite 30B) was obtained from Southern Clay Products (Gonzales, TX). Organoclays are produced by ion-exchange reactions, in which quaternary ammonium cations usually replace sodium cations between the galleries of montmorillonite (MMT)-type clays.[18] The cation-exchange capacity is 95 mequiv/100 g for all MMTs used in the Cloisite series. Cloisite 30B is an MMT modified with methyl tallow bis-2-hydroxyethyl quaternary ammonium cations (MMT-30B; data provided by the manufacturer). The Jeffamine-modified clays Somasif JAD230 and Somasif JAD400 were provided by the Freiburger Materialforschungszentrum (Freiburg, Germany). The characteristics of the nanoclays used in this study are listed in Table I.

Preparation

The nanocomposites were prepared by melt mixing in a laboratory kneader (type 50, Brabender, Duisburg, Germany). The mixing temperature was kept above 90°C, and this ensured proper melting of PEO. The PEOCNs were denoted by the type of clay: PEOCNC30, PEOCNJ400, and PEOCNJ230 contained 3 wt % Cloisite 30B, Somasif JAD400, and Somasif JAD230, respectively. For a better comparison, a pure PEO sample was also processed in the kneader to obtain a thermal history identical to that of the PEOCNs. Before mixing, the clays were dried in a vacuum oven at 70°C for 48 h. A mixing time of 20 min was used with a rotor speed of 30 rpm. In all cases, the torque stabilized to a constant value during this mixing time. Further, 100 mm × 100 mm × 1 mm (length × width × thickness) sheets were made by compression molding with a hot press (EP-Stanzteil, Wallenhorst, Germany) at a temperature of 100°C. The specimens for various tests were cut from the sheets at random.

Dynamic mechanical analysis (DMA)

DMA was performed for PEOCNs. Specimens were cut from the compression-molded sheets with dimensions of 20 mm × 8 mm × 1 mm (length × width × thickness) and tested in a Q800 dynamic mechanical thermal analysis (DMTA) instrument (TA Instruments, New Castle, USA) operating in a tensile testing mode. The test specimen was cooled to −120°C, allowed to stabilize, and then heated at a rate of 3°C/min to room temperature. The frequency of oscillation was fixed at 1 Hz. The storage modulus (E') and mechanical loss modulus (E'') were determined during the test and plotted against the temperature.

TABLE I
Characteristics of the Nanofillers

Organoclay	Interlayer distance	Structure
Cloisite 30B[a]	18.5 Å	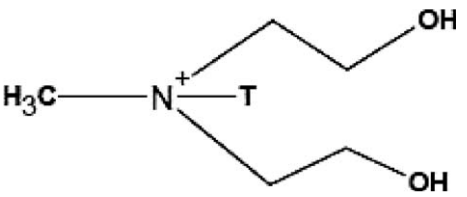
Somasif JAD230[b]	1.3 nm	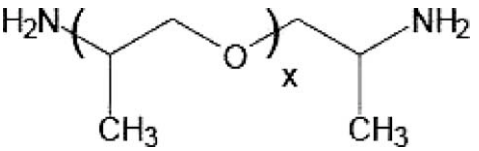
Somasif JAD400[c]	1.7 nm	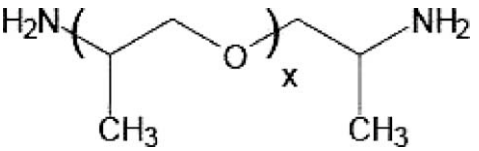

[a] T in the structure indicates tallow (~ 65% C1, ~ 30% C16, and ~ 5% C14).
[b] Molecular weight = 230.
[c] Molecular weight = 400.

Scanning electron microscopy (SEM)

The morphology of PEOCNs was investigated with a Zeiss (Oberkochen, Germany) Supra 40 VP scanning electron microscope. The compression-molded samples were quenched in liquid nitrogen and cryogenically ruptured to obtain cross sections, which were sputter-coated with carbon to avoid charging before SEM observation.

Atomic force microscopy (AFM)

A Nanoscope III atomic force microscope (Digital Instruments, Santa Barbara, CA), equipped with a microfabricated silicon cantilever with an integral tip (tapping-mode tip), was used to perform AFM imaging on the surfaces of compression-molded specimens, which were formed with two parallel glass plates to get a smooth surface.

Rheological measurements

Viscoelastic properties of PEOCNs were studied with a strain-controlled rheometer (ARES, Rheometric Scientific, Piscataway, NJ) equipped with 25-mm-diameter stainless steel parallel disks. Measurements were performed in an oscillatory shear configuration at 80°C. Test specimens were prepared by compression molding of the melt-intercalated composite from the kneader at 100°C for about 5 min into 2-mm-thick and 25-mm-diameter discs. For linear viscoelastic measurements, the dynamic strain sweep measurements were carried out first to determine the linear region. In oscillatory shear experiments, a sinusoidal shear strain [$\gamma(t)$] was imposed:

$$\gamma(t) = \gamma_0 \sin(\omega t)$$

where γ_0 is the strain amplitude, ω (0.1–500 rad/s), is the angular frequency, and t is the time. In the frequency sweep measurements, the frequency dependent (G') and complex viscosity (η^*) were determined.

Differential scanning calorimetry (DSC) analysis

The thermal behavior of PEO and PEOCNs was studied with a differential scanning calorimeter (DSC821, Mettler–Toledo, Greifensee, Switzerland). All the samples were dried before the measurements and analyses were carried out in a nitrogen atmosphere with standard aluminum pans. An approximately 10-mg sample was placed in an aluminum pan and heated from room temperature (25°C) to 90°C at a heating rate of 10°C/min. The melted sample was then cooled to 25°C at a cooling rate of 10°C/min. The reference was an empty aluminum pan.

Polarized optical microscopy (POM)

The formation of spherulites during the crystallization of PEO and PEOCNs was observed with a polarized optical microscope (Leica, Wild Leitz

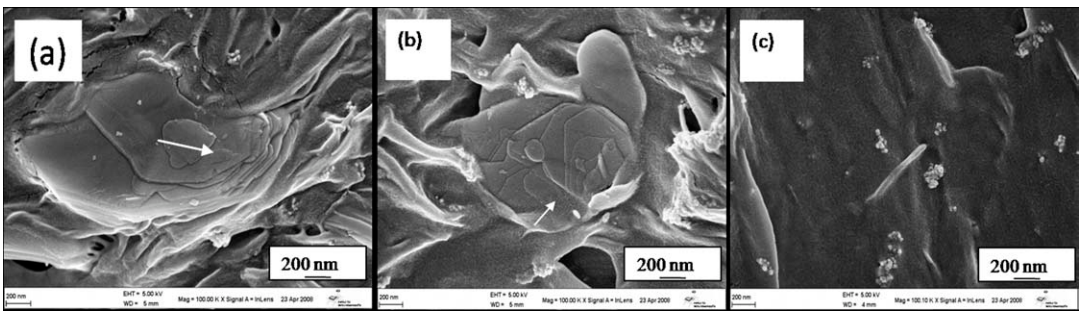

Figure 1 SEM images of freeze-fractured x–y plane surfaces of (a) PEOCNJ400, (b) PEOCNJ230, and (c) PEOCNC30 (all under 100,000× magnification). The arrows indicates the formation of intercalated layers.

GmbH, Ulm, Germany) equipped with a hot-stage unit (TMS 91, Linkam Scientific Instruments, Ltd., Waterfield, England). Thin specimens (layer thickness ~ 40 μm) were cut with a microtome. Crystallization was observed while the samples were exposed to the following temperature scans: heating at a rate of 10°C/min to 100°C, holding for 5 min to erase the thermal history effects, and then cooling to 40°C at a slow cooling rate of 2°C/min, during which the crystallization took place. The spherulites were viewed between crossed polarizers.

Tensile testing

The tensile properties of the samples were determined with dumbbell-shaped specimens (S3A type) with a Zwick (Ulm, Germany) 1474 universal testing machine according to the DIN 53504 test procedure. The length between the jaws was fixed at 40 mm, and at least five parallel measurements were performed to determine the mean values. Tests were run at room temperature at a crosshead speed of 1 mm/min, and the related modulus and strength values were determined.

RESULTS AND DISCUSSION

In most of the nanocomposite preparation methods, polymer/inorganic systems do not possess favorable thermodynamics for nanocomposite formation. The nanoclay can be trapped in dispersed or even exfoliated structures through solvent casting, sonication, or high-shear-rate/high-temperature extrusion. Such trapped structures are usually easy to achieve but in most cases are not thermodynamically stable or amenable to further processing. The melt-intercalation nanocomposite preparation method involves the mechanical mixing of a polymer with an appropriately modified filler and subsequent annealing above the softening temperature of the polymer.[32] This approach provides the best route for testing with sensitivity the thermodynamic arguments and yields well-defined systems for fundamental studies.[33] SEM was used to study the morphology of the intercalated clay structure, and photographs of the fractured surfaces of the PEOCNs are shown in Figure 1. The formation of an intercalated layered silicate structure was observed for PEOCNJ400 and PEOCNJ230. Because of the structural similarities of these nanoclays with PEO, there was a strong specific interaction that led the polymer to enter the clay layers, and this resulted in an intercalated layered silicate structure. Instead, the presence of a few agglomerates could be seen in the case of PEOCNC30, and this may have been due to poor interaction. This result is well supported by the AFM images shown in Figure 2. The bright phase represents the stiffer layered silicate, whereas the dark background represents the softer PEO matrix. Individual layers could not be seen very clearly by AFM, but they could be analyzed by TEM. However, intercalated structure formation was clear in the case of PEOCNJ400 and PEOCNJ230. On the basis of AFM studies, Zhang and Archer[34] proposed that partial flocculation occurs during thermal annealing and that, without pre-annealing, the PEO/silica nanocomposite structure is not thermodynamically stable in the melt state. Stefanescu et al.[35] reported the multilayered structure of PEO/MMT nanocomposite films made from solution. AFM suggests that excess polymer which is not directly adsorbed by the clay is wrapped around the stacked platelets and builds blobs, and the polymer also interconnects the polymer–clay layers.

In order to obtain deep knowledge about the effects of modifiers on the thermomechanical properties of composites, we discuss here the dynamic mechanical properties and rheology of the nanocomposites. The storage modulus and loss modulus of PEO and PEOCNs are shown in Figure 3. The presence of the nanoclay offered a considerable reinforcing effect, as was evident from the significant increase in E'. It can also be observed from the figure that the enhancement of E' in the case of PEOCNJ400 and PEOCNJ230 was higher than that in the case of PEOCNC30. It is well known that the reinforcement

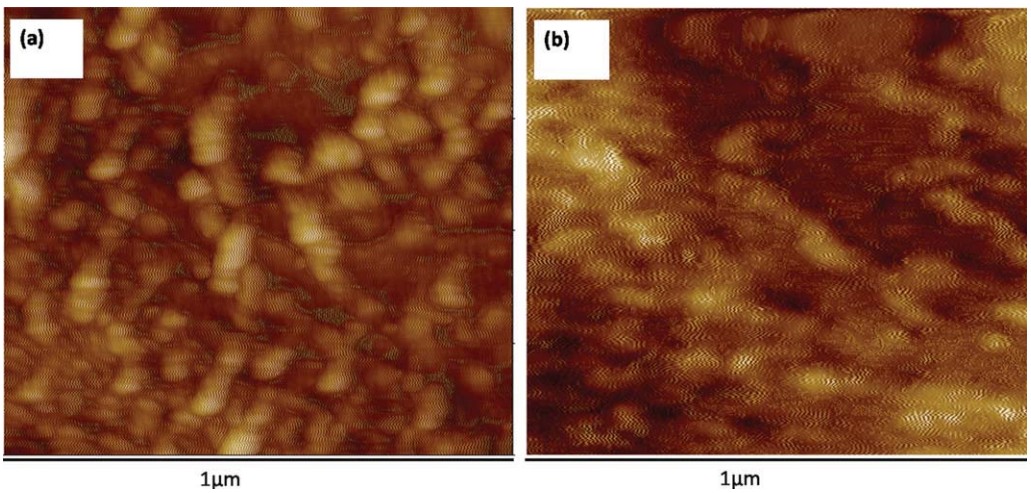

Figure 2 Representative AFM images from the *x–y* plane sections of films of (a) PEOCNJ230 and (b) PEOCNJ400. [Color figure can be viewed in the online issue, which is available at www.interscience.wiley.com.]

effect increases with better intercalation of the polymer in the clay layers. The structural similarities of PEO and the nanoclays (JAD400 and JAD230) were noteworthy and enabled better intercalation.

It is also interesting that PEOCNJ400 and PEOCNJ230 displayed higher E'' values than neat PEO, whereas PEOCNC30 reduced the loss. The higher damping loss could be explained by a phenomenon similar to the constrained layer damping (CLD) concept.[36] When a viscoelastic layer is constrained between two rigid layers, the damping efficiency or loss of the viscoelastic material increases, so the increase in E'' of PEOCNJ400 and PEOCNJ230 can be well explained. The better intercalation of the nanoclay in the polymer matrix can be considered to form a large number of nano-CLD systems in which the nanoclay acts as constraining layers and PEO forms the viscoelastic layer. The reinforcing effect due to better intercalation of JAD400 and JAD230 is also reflected in the tensile properties of PEOCNs (Fig. 4). The tensile modulus of PEOCNC30, PEOCNJ230, and PEOCNJ400 was enhanced by 13, 26, and 31%, respectively. Similarly, the tensile strength of PEOCN30, PEOCNJ230, and PEOCNJ400 was also enhanced by 4, 22, and 9%, respectively. The filler–matrix interface is the critical factor determining to what extent the potential properties of a composite will be achieved and maintained during use. From the AFM and SEM micrographs, it is clear that PEOCNJ230 had better interactions than the other nanoclays used in this study and hence better mechanical properties. Yung et al.[37] reported the modeling of Young's modulus of polymer-layered silicate nanocomposites with a modified Halpin–Tsai micromechanical model as a function of the clay concentration for various parametric variations, including the exfoliation ratio, the particle/matrix stiffness ratio, the particle volume fraction, and the particle aspect ratio. In comparison with other thermoplastic polymers, there are fewer reports on the mechanical and dynamic mechanical properties of PEO-based materials because they are not used for high-strength applications. Recently, Ratna et al.[21] reported that the incorporation of ions into PEO for

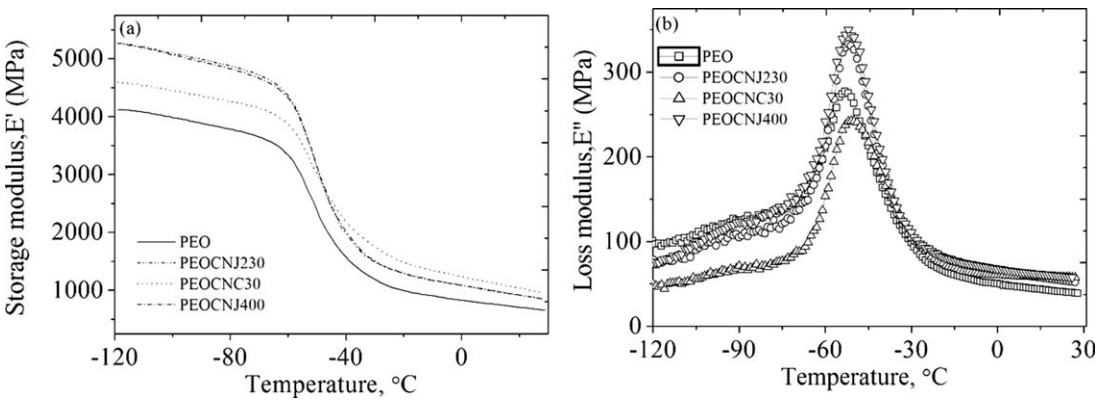

Figure 3 Dynamic mechanical properties of PEOCNs with different types of nanoclays: (a) E' versus the temperature and (b) E'' versus the temperature.

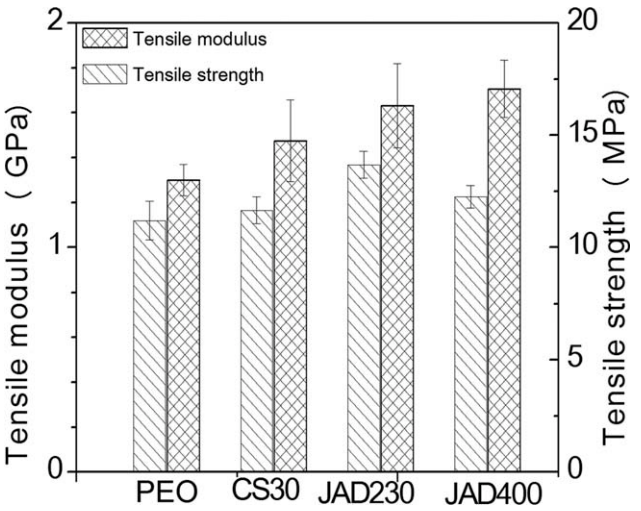

Figure 4 Variation of the tensile properties of PEOCNs with different types of nanoclays.

solid polymer electrolyte applications reduced the strength of PEO substantially, and some sort of reinforcement and mechanical analysis are very important for the development of high-performance PEO-based solid polymer electrolyte applications.[19–22] We also observed that the elongation at break slightly decreased for the PEOCN systems. The reduction in the PEOCNs may have been due to the presence of stacked silicate layers. A similar trend has been observed and reported for thermoplastic nanocomposites such as intercalated poly(methyl methacrylate) and polystyrene and intercalated–exfoliated polypropylene.[38–40] Fornes et al.[41] reported similar behavior of increasing modulus and decreasing elongation at break for a nylon 6 matrix in a nylon 6/layered silicate nanocomposite system.

Figure 5 shows the viscosities of PEO and PEOCNs measured at 80°C. The curves are typically pseudoplastic in nature; that is, when the temperature was kept constant, the shear viscosities decreased with respect to the shear rate. It is also evident from Figure 5 that η* and G' of the nanocomposites at a low shear rate were much higher than those of the pure PEO. The enhancement in η* is often explained in terms of the confinement of polymer chains within the silicate layer.[42,43] The viscosity of the confined polymer melt is always greater than that of the bulk. The higher viscosity of the confined melt is believed to arise from an immobilized hydrodynamic layer near the wall having a thickness of the order of the radius of gyration of the polymer chain. It is clear from the figure that the increases in η* and G' of the PEOCNs were almost even in comparison with PEO, regardless of the type of nanoclay reinforcement used. This is, however, different from the E' behavior obtained from the aforementioned DMTA measurements. The DMTA measurements were performed at a temperature (−120 to 25°C) well below the melting point of PEO (68°C), whereas rheological studies were carried out at 80°C (above the melting temperature of the matrix).

It is expected that the incorporation of nanoparticles into a semicrystalline polymer matrix will substantially affect the crystallization behavior of the polymer. There can be three general behaviors during crystallization depending on the polymer–filler interactions: the development of new crystal structures, heterogeneous nucleation by fillers, and polymer amorphization by fillers.[44] POM was used to compare the crystal morphology of PEO and PEOCNs. Figure 6 presents POM images of PEO and PEOCNs that were isothermally crystallized at 40°C. The morphology of the crystals is shown during the final stage of crystallization. For PEO alone, the spherulites were similar in size. For PEOCNs, the spherulites were smaller than those seen in the virgin PEO. Similar behavior was reported by

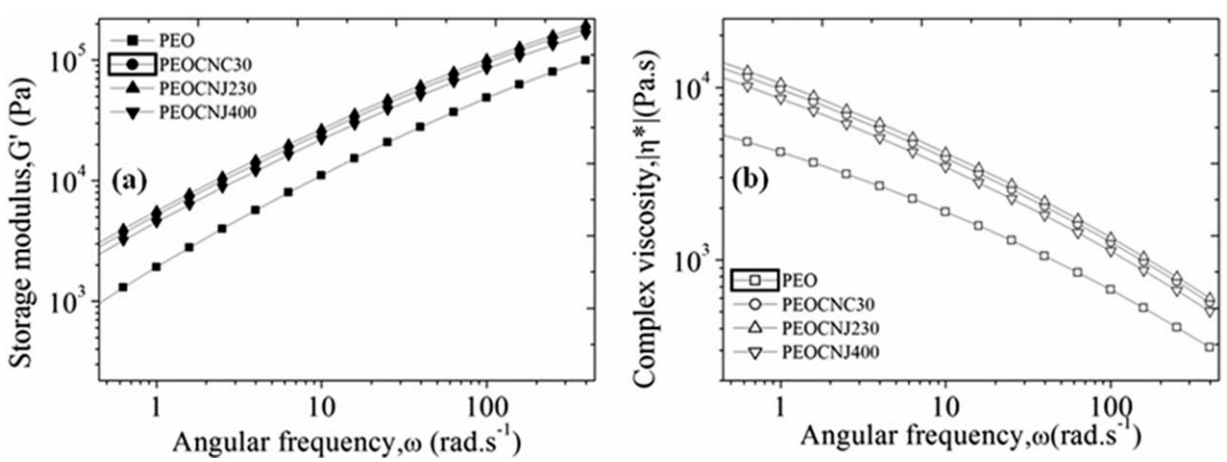

Figure 5 Frequency responses of PEOCNs with fixed molecular weights and particle volume fractions but various types of nanoclays: (a) G' and (b) η*. Measurements were carried out at 80°C with a strain amplitude of 10%.

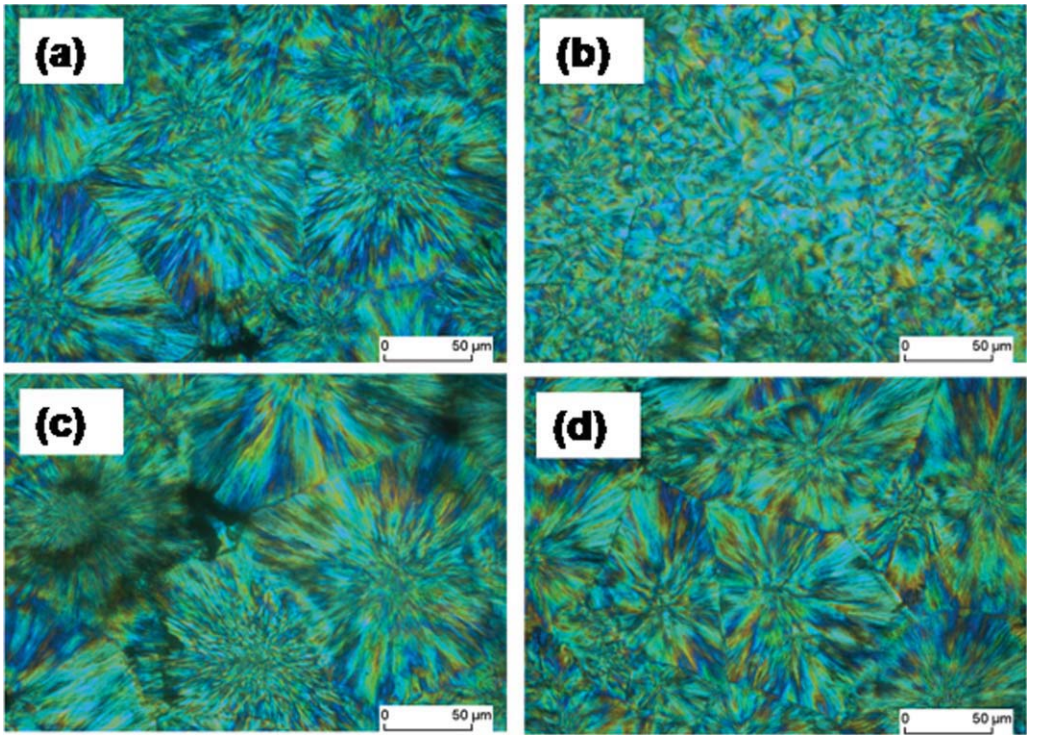

Figure 6 Cross-polarization optical microscopy images after complete crystallization (spherulites were recorded by the melt being cooled to 40°C at the slow cooling rate of 2°C/min and being held there for 60 min): (a) PEO, (b) PEOCNC30, (c) PEOCNJ400, and (d) PEOCNJ230. [Color figure can be viewed in the online issue, which is available at www.interscience.wiley.com.]

Strawhecker and Manias[45] and also by Ratna et al.[20] for solution-intercalated PEOCN systems. It is also clear from Figure 6 that the spherulite size of PEOCNC30 was greatly reduced in comparison with other PEOCNs and the PEO matrix itself. This behavior originated from the discontinuity of space caused by the agglomerates, which forced the spherulites to have sizes comparable to the filler–filler separation, independently of the bulk polymer spherulite size. The formation of clay tactoids on the fractured surface was observed in SEM photographs in the case of PEOCNC30, as already discussed. These agglomerates may have been acting as nucleating agents and resulted in a different crystalline morphology in comparison with PEO. As the number of nucleation sites increased, the number of spherulites also increased, and hence smaller spherulites formed. On the other hand, in PEOCNJ400 and PEOCNJ230, the spherulite size was not so much reduced, as there were no agglomerates to hinder spherulite growth.

In Table II, we compare the DSC crystallization plots of PEO and PEOCNs. We found that for the composites, the crystallization peak temperature was unaffected (Fig. 7). A slight increase in the

TABLE II
Crystallization Characteristics of PEOCNs

Sample	Peak melting temperature (°C)	Enthalpy of crystallization (J/g)	Degree of crystallinity (%)
PEO	68.1	136	66
PEOCNC30	70.1	151	71
PEOCNJ400	72.5	146	69
PEOCNJ230	73.1	144	68

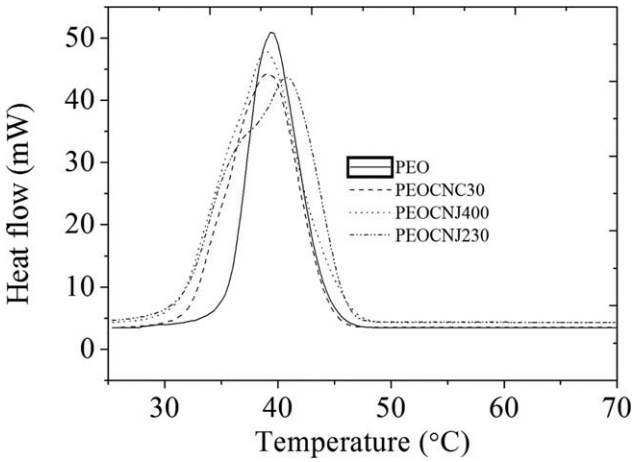

Figure 7 DSC traces of different PEOCNs. The melted samples were cooled to room temperature at the cooling rate of 10°C/min.

crystallization peak temperature of PEOCNJ230 may have been due to the well-dispersed nanoclay, as evidenced by SEM and AFM images. The heat of crystallization of PEOCNs increased in comparison with the PEO matrix, and this indicated that the nanoclay acted as the nucleating center. The heat of crystallization was greater in the case of PEOCN30 versus PEOCNJ230 and PEOCN400 as the number of crystals formed was greater; this was evident from the POM micrographs. The crystallinity percentage of PEO was enhanced marginally by the incorporation of nanoclay. As expected, the crystalline fraction percentage was also greater in the case of PEOCNC30, whereas there was only marginal improvement in the case of PEOCNJ230 and PEOCNJ400. Despite a great difference in the number of crystallites between the PEO matrix and PEOCNC30, the crystalline fraction did not show a marked change between these two systems. The melting peak temperature of the composite increased with respect to PEO, and this could be attributed to the different crystalline structures formed during the melt-mixing process. These interesting peculiarities will be investigated in more detail in the future.

CONCLUSIONS

PEO-layered silicate nanocomposites were prepared with different reinforcing nanoclays (Cloisite 30B, Somasif JAD400, and Somasif JAD230) at a concentration of 3 wt % by simple melt mixing with a laboratory kneader followed by compression molding. The characterization of the nanocomposites by AFM and SEM showed the formation of intercalated structures for PEOCNJ230 and PEOCNJ400. The incorporation of Cloisite 30B into PEO caused retardation of the crystal growth and resulted in smaller and irregular spherulites, whereas in the case of PEOCNJ230 and PEOCNJ400, the spherulites were found to be identical to those of PEO. This observation was well supported by the DMTA results; the presence of the nanoclay produced a considerable reinforcing effect, as was evident from a significant increase in E'. The enhancement of E' in the case of PEOCNJ400 and PEOCNJ230 was higher (identical spherulites) than that in the case of PEOCNC30 (smaller and irregular spherulites). The increase in η^* and G' of the PEOCNs was comparable, regardless of the type of nanoclay reinforcement used. This was, however, different from the E' variation obtained from the aforementioned DMTA measurements. It is noteworthy to recall that the DMTA measurements were performed at a temperature (-120 to 25°C) well below the melting point of PEO (68°C), whereas rheological studies were carried out at 80°C (above the melting temperature of the matrix). There was no significant change in the crystallization temperature of the PEOCNs, whereas the crystalline fraction percentage was greater in the case of PEOCNC30, and there was only marginal improvement in the case of PEOCNJ230 and PEOCNJ400.

References

1. Pinnavaia, T. J.; Beall, G. W. Polymer–Clay Nanocomposites; Wiley: Chichester, United Kingdom, 2000.
2. Alexandre, M.; Dubois, P. Mater Sci Eng 2000, 28, 1.
3. Kawasumi, M. J Polym Sci Part A: Polym Chem 2004, 42, 819.
4. Nguyen, Q. T.; Baird, D. G. Adv Polym Technol 2006, 25, 270.
5. Ratna, D.; Manoj, N. R.; Singh Raman, R. K.; Varley, R.; Simon, G. P. Polym Int 2003, 52, 1403.
6. Vaia, R. A.; Jandt, K. D.; Kramer, E. J.; Giannelis, E. P. Macromolecules 1995, 28, 8080.
7. Becker, O.; Cheng, Y. B.; Varley, R. J.; Simon, G. P. Macromolecules 2003, 36, 1616.
8. Lan, T.; Kaviratna, P. D.; Pinnavaia, T. J. J Phys Chem Solids 1996, 57, 1005.
9. Alcantar, N. A.; Aydil, E. S.; Israelachvili, J. N. J Biomed Mater Res 2000, 51, 343.
10. Yang, X. Q.; Hanson, L.; McBreen, J.; Okamoto, Y. J Power Sources 1995, 54, 198.
11. Mishra, R.; Rao, K. J. Solid State Ionics 1998, 106, 113.
12. Aranda, P.; Mosqueda, Y.; Perez-Cappe, E.; Ruiz-Hitzky, E. J Polym Sci Part B: Polym Phys 2003, 41, 3249.
13. Kuo, S. W.; Lin, C. L.; Chang, F. C. Macromolecules 2002, 35, 278.
14. Talibuddin, S.; Wu, L.; Runt, J.; Lin, J. S. Macromolecules 1996, 29, 7527.
15. Ratna, D.; Divekar, S.; Samui, A. B.; Chakraborty, B. C.; Banthia, A. K. Polymer 2006, 47, 4068.
16. Vaia, R. Nat Mater 2005, 4, 429.
17. Aranda, P.; Ruiz-Hitzky, E. Acta Polym 1994, 45, 59.
18. Shen, Z.; Simon, G. P.; Cheng, Y. B. Polymer 2002, 43, 4251.
19. Aranda, P.; Ruiz-Hitzky, E. Acta Polym 1994, 45, 59.
20. Ratna, D.; Divekar, S.; Samui, A. B.; Chakraborty, B. C.; Banthia, A. K. Polymer 2006, 47, 4068.
21. Ratna, D.; Divekar, S.; Sivaraman, P.; Samui, A. B.; Chakraborty, B. C. Polym Int 2007, 56, 900.
22. Kwiatkowski, J.; Whittaker, A. K. J Polym Sci Part B: Polym Phys 2001, 39, 1678.
23. Hackett, E.; Manias, E.; Giannelis, E. P. Chem Mater 2000, 12, 2161.
24. Kim, T. H.; Jang, L. W.; Lee, D. C.; Choi, H. J.; Jhon, M. S. Macromol Rapid Commun 2002, 23, 191.
25. Krishnamoorti, R.; Yurekli, K. Curr Opin Colloid Interface Sci 2001, 6, 464.
26. Yang, D. K.; Zax, D. B. J Chem Phys 1991, 110, 5325.
27. Malwitz, N. M.; Dundigalla, A.; Ferreiro, V.; Butler, P. D.; Henk, M. C.; Schmidt, G. Phys Chem Chem Phys 2004, 6, 2977.
28. Chen, B.; Evans, J. R. G. J Phys Chem B 2004, 108, 14986.
29. Bonderer, L. J.; Studart, A. R.; Gauckler, L. J. Science 2008, 319, 1069.
30. Loizou, E.; Butler, P.; Porcar, L.; Schmidt, G. Macromolecules 2006, 39, 1614.
31. Abraham, T.; Ratna, D.; Siengchin, S.; Karger-Kocsis, J. Polym Eng Sci 2008, 49, 379.
32. Vaia, R. A.; Ishii, H.; Giannelis, E. P. Chem Mater 1993, 5, 1694.
33. Vaia, R. A.; Giannelis, E. P. Macromolecules 1997, 30, 8000.
34. Zhang, Q.; Archer, L. A. Langmuir 2002, 18, 10435.

35. Stefanescu, E. A.; Dundigalla, A.; Ferreiro, V.; Loizou, E.; Porcar, L.; Negulescu, I.; Garnoa, J.; Schmidt, G. Phys Chem Chem Phys 2006, 8, 1739.
36. Wheeler, M. E. U.S. Pat. 6,110,985 (2000).
37. Yung, K. C.; Wang, J.; Yue, T. M. J Reinforced Plast Compos 2006, 25, 847.
38. Lee, D. C.; Jang, L. W. J Appl Polym Sci 1996, 61, 1117.
39. Lee, D. C.; Jang, L. W. J Appl Polym Sci 1998, 68, 2005.
40. Noh, M. W.; Lee, D. C. Polym Bull 1999, 42, 619.
41. Fornes, T. D.; Yoon, P. J.; Keskkula, H.; Paul, D. R. Polymer 2001, 42, 9929.
42. Subbotin, A.; Semenov, A.; Doi, M. Phys Rev E 1997, 56, 623.
43. Khare, R.; Pablo, J.; Yethiraj, A. M. Macromolecules 1996, 29, 7910.
44. Manias, E.; Polizos, G.; Nakajima, H.; Heidecker, M. J. Fundamentals of Polymer Nanocomposite Technology in Flame Retardant Polymer Nanocomposites; Wiley: Hoboken, NJ, 2007; p 31.
45. Strawhecker, K. E.; Manias, E. Chem Mater 2003, 15, 844.